Solar Energy Materials and Solar Cells 174 (2018) 433–444

Contents lists available at ScienceDirect

Solar Energy Materials and Solar Cells

journal homepage: www.elsevier.com/locate/solmat

High stability of benzotriazole and benzodithiophene containing medium band-gap polymer solar cell

Hande Unay[a], Gisele A. dos Reis Benatto[b], Michail J. Beliatis[b], Suren A. Gevorgyan[b], Pelin Kavak[c], Sema Memiş[d], Ali Cirpan[a,e,f,g], Levent Toppare[a,e,f], Elif Alturk Parlak[d,*], Frederik C. Krebs[b]

[a] Department of Polymer Science and Technology, Middle East Technical University, 06800 Ankara, Turkey
[b] Department of Energy Conversion and Storage, Technical University of Denmark, Frederiksborgvej 399, 4000 Roskilde, Denmark
[c] Yildiz Technical University, Physics Department, 34220 Esenler, Istanbul, Turkey
[d] TÜBİTAK MAM Material Institute, Photonic and Electronic Sensors Laboratory, 41470 Gebze, Kocaeli, Turkey
[e] Department of Chemistry, Middle East Technical University, 06800 Ankara, Turkey
[f] The Center for Solar Energy Research and Application (GUNAM), Middle East Technical University, 06800 Ankara, Turkey
[g] Department of Micro and Nanotechnology, Middle East Technical University, 06800 Ankara, Turkey

ARTICLE INFO

Keywords:
P-SBTBDT
Inverted organic solar cell
OPV
Stability
ISOS
Encapsulation
Life time evaluation testing
Degradation
Benzotriazole
Selenophone

ABSTRACT

The improvement of polymer solar cell stability is a challenge for the scientists and has significant implications commercially. In this study, we investigated the stability of a novel P-SBTBDT active material applied in an inverted type solar cell. Detailed stability experiments comprising shelf life, laboratory weathering and outdoor testing were carried out according to ISOS testing guidelines. Shelf life showed that P-SBTBDT solar cells were very stable after 840 h with encapsulation. Although accelerated weathering aging tests are a very harsh, the devices remained stable after the burn-in phase with T_{50} from 700 to 840 h, with some P-SBTBDT solar cells did not reach T_{50} in the time span of the test. Degradation tests on the P-SBTBDT solar cells which were carried out under natural solar light indicated that T_{40} was reached after 840 h. The results of dark, light, damp and dry stability tests showed that most of the degradation was provoked by failure of the encapsulation. The experiments indicated that P-SBTBDT solar cells are sensitive to light and oxygen but are strikingly stable under humid conditions. Further developments for minimizing the degradation effects using UV-filters and better encapsulation are some of the necessary improvements in further research.

1. Introduction

Polymer solar cells (PSCs) are attracting significant attention at present since they are renewable materials to produce electricity with light weight, and relatively low cost of production [1–4].

Inverted type polymer solar cells show better long-term stability compared to normal device geometry polymer solar cells since there is no need for the acidic hole-transporting layer; poly(3,4-ethylenedioxylenethiophene):poly(styrenesulfonic acid) (PEDOT:PSS) and low-work-function metal cathodes which reduce device lifetime [5–8]. Vertical phase separation in the active layer is a superior advantage for inverted solar cells, since it leads to more efficient exciton dissociation [9]. This can be considered as a self-encapsulated device since durable metals are used as the top electrode [10]. It is quite challenging to fabricate PSCs that yield high power conversion efficiency (PCE) while retaining good ambient stability [11].

Degradation of OPVs is a complicated issue and is not yet fully understood. There are a variety of factors that affect the stability of OPVs. Chemical reactions between O_2 and H_2O molecules and the active layer and electrode materials. Diffusion of electrode materials and their reactions with the active layer, delamination of the cathode, nano-phase modifications and photo-oxidation of the active layer [12] also contribute to the overall degradation of OPVs. Furthermore, many of these degradation mechanisms are interrelated; creating additional complications in understanding the overall degradation process [13–15].

Oxygen (O_2) and humidity can diffuse through grain boundaries and pinholes into the device and deteriorate polymer/organic materials. Since metal electrodes are in direct contact with the active layer, the metal can penetrate and react with the active layer. To eliminate this effect, metal oxides are used as buffer layers between the polymer and metal electrode where their use improves the device durability [16–19]. The main drawback of conventional polymer solar cells is rapid

* Corresponding author.
E-mail address: elif.parlak@tubitak.gov.tr (E.A. Parlak).

http://dx.doi.org/10.1016/j.solmat.2017.09.024
Received 10 October 2016; Received in revised form 26 August 2017; Accepted 12 September 2017

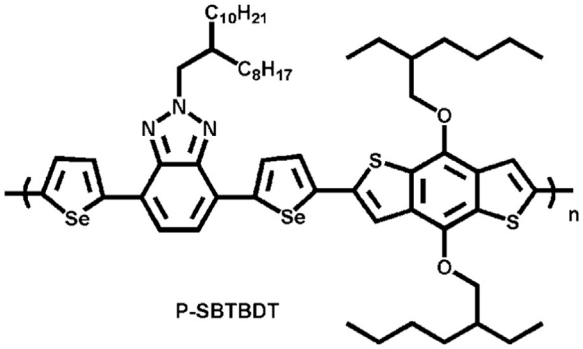

Scheme 1. Synthetic pathway and chemical structure of **P-SBTBDT**.

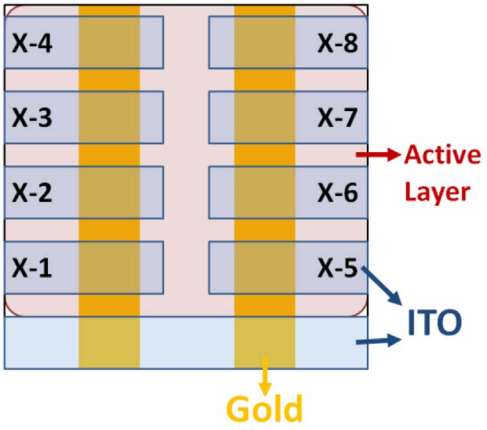

Fig. 1. Module design and cells identification. X represents the name of the sample.

oxidation/water reaction of the aluminum (Al) electrode [20]. Inverted solar cells are a good approach to solve this problem since the architecture uses the ability to reverse the polarity of charge collection [21–28]. Instead of an aluminum electrode, metals such as silver (Ag) or gold (Au) are used for the electrodes in inverted structure solar cells. Titanium oxide (TiO_2), Zinc oxide (ZnO) among others can be used as the buffer layers between polymer and metal electrode.

Medium band gap polymers can also be used for the fabrication of PSCs. These can be designed with a suitable donor (D) and acceptor (A) segments in the polymer chain and with high LUMO level acceptors [29–31]. In this letter, selenophone units were inserted between benzotriazole (BTz) and dialkoxyl-substituted benzo [1,2-b:4,5- b′]dithiophene (BDT) molecules which provided high mobility and improved photon harvesting (Fig. 2a). Selenophene substitution facilitated the development of conductivity and mobility due to Se-Se intermolecular interactions. Selenophene containing polymers indicated a good planarity and an extended conjugation length. Selenophene containing polymers compared to other chalcogeophene derivatives exhibit lower band gap, since LUMO level is deeply reduced, whereas HOMO is not changed [32–34]. Moreover,

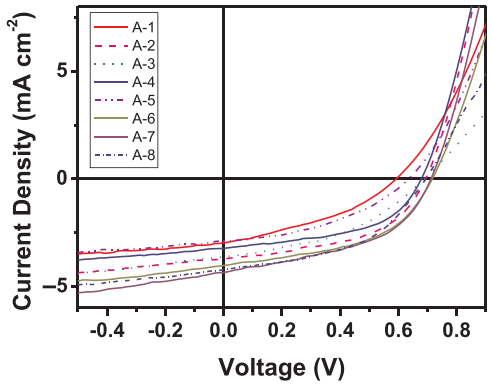

Fig. 3. IV-characteristics of inverted **P-SBTBDT** solar cells without post annealing (devices are A-1 to A-8).

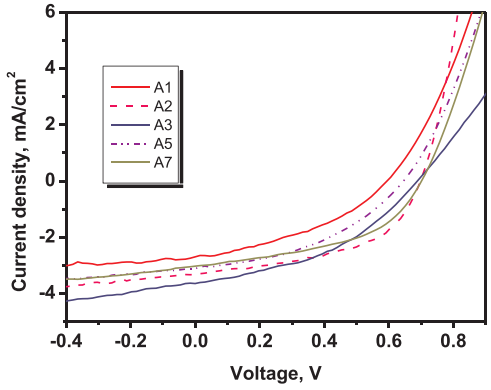

Fig. 4. IV-characteristics of inverted **P-SBTBDT** solar cells after post annealing (devices are P A-1 to P A-7).

selenophene, BDT, BTz containing polymers have high hole mobilities.

In this paper, we investigated the stability of novel P-SBTBDT solar cells. The stability measurements were carried out according to the ISOS protocols [35]. ISOS protocols are a set of guidelines that explain the procedures of organic solar cell stability measurements under different test conditions. Laboratory indoor (ISOS-L-1, ISOS-L-2, ISOS-L-3, ISOS-D-1, ISOS-D-3) and outdoor tests (ISOS O-1) of PSCs were performed in order to unveil and address the weak points in the device durability. With further development, it is expected that P-SBTBDT solar cell will approach the goal of 10000 h lifetime under outdoor conditions.

2. Experimental

2.1. Materials

Polymer (Scheme 1) were synthesized with the route reported previously [36]. n-Type semiconductor phenyl-C_{71}-butyric acid methyl

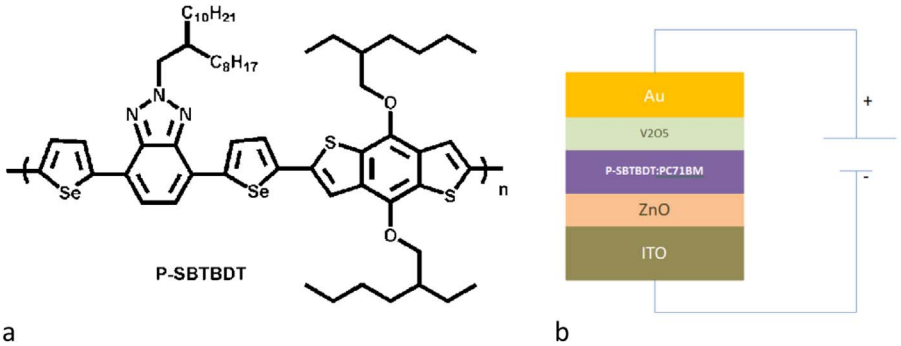

Fig. 2. a) Chemical structure of **P-SBTBDT**, b) Inverted solar cell architecture **P-SBTBDT** solar cells.

Table 1
Brief of ISOS Protocols.

	ISOS-D-1	ISOS-D-3	ISOS-L-1	ISOS-L-2	ISOS-L-3	ISOS-O-1
Light source	None	None	Simulator AM 1.5G	Simulator AM 1.5G	Simulator AM 1.5G	The sun light
Temperature	Ambient	65 °C	Ambient	65 °C	65 °C	Ambient outdoor
Relative humidity	Ambient (low)	85% (chamber)	Ambient (low)	Ambient (low)	Controlled (50%)	Ambient outdoor
Characterization İon light source	Solar simulator	Solar simulator	Solar simulator	Solar simulator	Solar simulator	Solar simulator

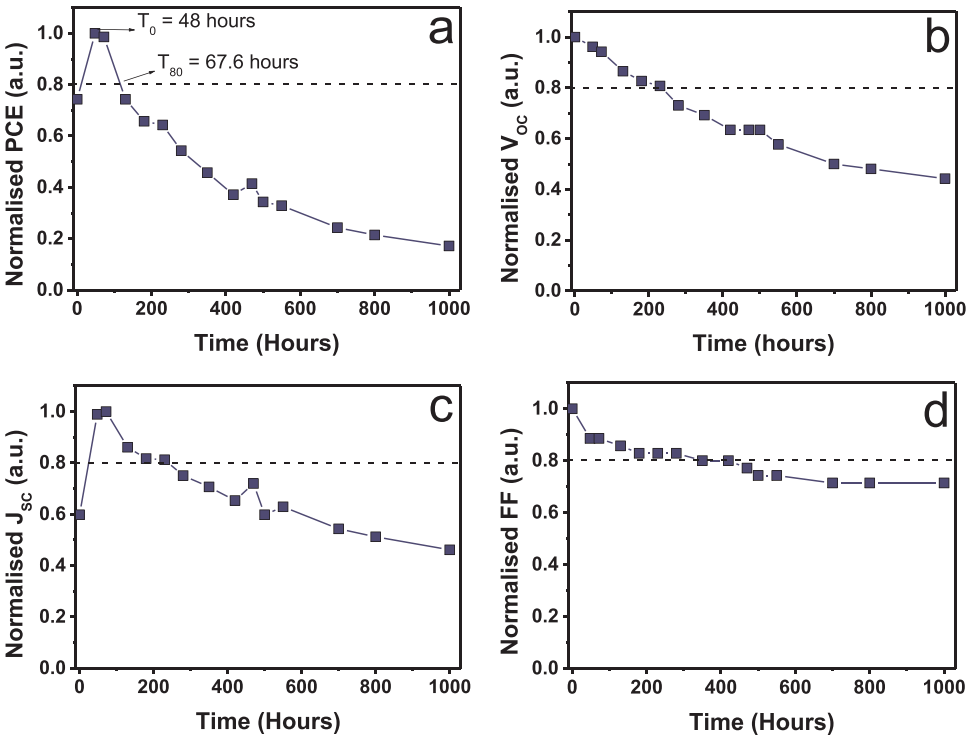

Fig. 5. Normalised stability of **P-SBTBDT** solar cells of a) PCE; b) V_{OC}; c) J_{SC}; and d) FF vs time plot after 1000 h under ISOS-L-1 test.

ester ($PC_{71}BM$) was purchased from Sigma-Aldrich. PCDTBT and PCBM solutions were prepared using 1,2-dichlorobenzene obtained from Alfa Aesar.

2.2. Characterization

The current density–voltage (J–V) characteristics of devices were taken using standard solar irradiation of 1000 Wm^{-2} (AM1.5G) with xenon lamp as the light source and computer-controlled voltage–current Keithley 2600 source meter at 25 °C under ambient atmosphere. Morphology of the blend films were investigated by Atomic Force Microscopy (AFM) (Park Systems). The stability tests of DTU were performed in the Characterization Laboratory for Organic Photovoltaics (CLOP) at the Department of Energy Conversion and Storage, DTU, Roskilde, Denmark. For ISOS-D-1 the devices were stored in a shelf at ambient humidity and temperature. For ISOS-D-3 the samples were placed in a damp heat chamber (from Thermotron) set at 85% relative humidity (RH) and 65 °C air temperature. For ISOS-L-3 a weathering chamber (Q-Lab) containing a xenon lamp was set to 85 °C device temperature (black panel), 50% RH and illumination of around 0.7 Sun. In ISOS-L-2 the experiment was carried out at a monitored temperature of 65 °C under a solar simulator. In ISOS-O-1 the samples were placed on a solar tracker outside. The outdoor experiments started on February 17th, 2015 in Denmark. In all tests performed at DTU, the samples were periodically removed from the ageing setup and tested under a calibrated solar simulator with AM1.5G and 1000 W m^{-2} of illumination.

Table 2
Photovoltaic parameters of P-SBTBDT solar cells before and after post annealing.

Device	V_{OC} (V)	J_{SC} (mA/cm^2)	FF (%)	PCE (%)
A-1	0.59	2.98	0.37	0.65
A-2	0.69	3.72	0.49	1.28
A-3	0.69	3.64	0.42	1.04
A-4	0.68	3.23	0.51	1.11
A-5	0.64	2.89	0.41	0.75
A-6	0.71	4.02	0.49	1.40
A-7	0.71	4.35	0.46	1.44
A-8	0.69	4.23	0.48	1.40
P A-1	0.59	2.69	0.39	0.63
P A-2	0.69	3.32	0.50	1.17
P A-3	0.69	3.47	0.42	0.99
P A-4	0.69	3.64	0.42	1.04
P A-5	0.64	2.89	0.41	0.75
P A-6	0.71	3.23	0.42	0.98
P A-7	0.70	3.02	0.48	1.01
P A-8	0.69	3.10	0.31	0.66

2.3. Fabrication of polymer solar cells

P-SBTBDT solar cells were fabricated on indium tin oxide (ITO) coated glass substrates with a sheet resistance of 15 Ω/cm. The substrates were cleaned in an ultrasonic bath with acetone, isopropyl alcohol, and deionized-water, successively for 5 min; and dried under nitrogen flow. ZnO buffer layers were deposited with sputtering as 40 nm. Afterwards, a solution of **P-SBTBDT** and $PC_{71}BM$ (1:1) was prepared, and the resulting solution was spin-coated onto the ZnO

Table 3
Initial and final efficiency of the samples tested at DTU under different ISOS test conditions.

Module	Device	First PCE (%)	Last PCE (%)	ISOS test
1	1	0.487	0.000	**L-2**
	2	1.126	0.095	
	3	0.325	0.066	
	4	0.968	0.056	
	5	0.588	0.000	
	6	1.093	0.057	
	7	1.016	0.080	
	8	1.182	0.115	
2	1	0.851	0.374	**D-3**
	2	1.277	0.611	
	3	1.344	0.635	
	4	1.423	0.461	
	5	0.757	0.492	
	6	1.200	0.646	
	7	1.172	0.642	
	8	1.333	0.424	
3	1	1.118	0.349	**O-1**
	2	1.194	0.387	
	3	1.095	0.330	
	4	0.306	0.000	
	5	1.017	0.000	
	6	1.053	0.000	
	7	0.171	0.000	
	8	0.305	0.000	
4	1	0.852	0.176	**L-3**
	2	1.240	0.209	
	3	1.113	0.202	
	4	1.205	0.178	
	5	0.694	0.165	
	6	1.127	0.200	
	7	1.285	0.215	
	8	1.276	0.180	
5	1	0.149	0.051	**O1**
	2	1.044	0.005	
	3	1.265	0.000	
	4	1.489	0.000	
	5	0.074	0.000	
	6	0.048	0.000	
	7	1.052	0.000	
	8	1.369	0.000	
6	1	0.749	0.000	**L3**
	2	1.349	0.082	
	3	1.377	0.109	
	4	1.161	0.110	
	5	0.409	0.069	
	6	0.065	0.028	
	7	0.190	0.000	
	8	0.095	0.002	
7	1	0.460	0.096	**D1**
	2	0.658	0.362	
	3	1.126	0.492	
	4	0.483	0.037	
	5	0.090	0.147	
	6	1.123	1.154	
	7	0.729	0.964	
	8	0.073	0.110	
8	1	0.992	0.01	**L-2**
	2	1.334	0.046	
	3	1.340	0.085	
	4	1.443	0.123	
	5	1.026	0.083	
	6	1.140	0.073	
	7	1.113	0.070	
	8	0.000	0.000	

coated substrates. Finally, V_2O_5 (10 nm) and gold (80 nm) were deposited as the cathode layers by vacuum evaporation technique. The active area of the cell was 0.09 cm^2. The encapsulation of the polymer solar cell was performed using Ossila UV curing resin. The **P-SBTBDT** solar cell architecture is given in Fig. 2b.

The modules were built with 8 cells, sharing a common anode (ITO). The cells are identified as shown in Fig. 1.

3. Results and discussion

3.1. Device performance under illumination

Photovoltaic performances of inverted solar cells were investigated. We previously studied **P-SBTBDT** solar cells with a conventional configuration [36]. However, in this study we only fabricated inverted structure devices (Fig. 2b).

Inverted solar cells based on **P-SBTBDT** were manufactured and investigated. Figs. 3 and 4 show JV characteristics of the devices before and post annealing. Post annealing decreased the performance of **P-SBTBDT** solar cells from 1.13% to 0.90% mostly due to the decrease in the short current density (J_{SC}) values from 3.63 to 3.17 mA cm^{-2} where the fill factor FF decreased from 45% to 42%. No change was observed in open circuit voltage V_{OC}.

3.2. Stability tests of OPV devices

There are several categories of stability testing of OPV devices such as tests under dark, simulated light, humidity and at outdoor conditions. Each degradation test[35] is divided into three categories: basic (1), intermediate (2), advanced (3) levels. The main variables of the experiments are temperature, light, humidity and environment (Table 1).

The solar cells were tested with ISOS-D-1, ISOS-D-3, ISOS-L-1, ISOS-L-2, ISOS-L-3, ISOS-O-1 protocols [35]. The main parameters of the tests are listed in Table 1. The solar cells were exposed to ageing with different time spans following the aforementioned protocols. The recorded IV-curves under calibrated sun simulator were used to construct the degradation curves which were normalised to the maximum performance of the corresponding parameter, in order to show the real T_{80} in the case of photo annealing effects [37].

3.2.1. Stability testing in TÜBİTAK

The combination of sunlight and O_2 will deteriorate the polymeric materials and damage the electrical properties of organic solar cells. For indoor testing ISOS-L-1 was carried out to study degradation of the device under illumination and air. ISOS-L-1 testing indicated that the efficiencies and short circuit currents changed with time. Fig. 5 shows the stability curve of the inverted **P-SBTBDT** solar cell for 1000 h under solar simulator illumination. T_{80} is the time required for the cells to reach an efficiency of 80% of their starting value. As an example, T_{80} value of 235 h for P3HT polymer based devices was reported earlier in the literature [38]. In **P-SBTBDT** solar cells, after a photo annealing effect, T_{80} value is 67.6 h (Table 2). The conventional type PSC device based on **P-SBTBDT**: $PC_{71}BM$ (1:1, w/w) exhibited the best PCE of 3.60% with a V_{OC} of 0.67 V, a J_{SC} of 8.95 mA cm^{-2} and a FF of 60%. Both results supported that this polymer is very promising for solar cell technology.

3.2.2. Stability testing in DTU

The advanced long term stability testing of P-SBTBDT solar cells was carried out in the Technical University of Denmark (DTU). Shelf life and damp heat tests (ISOS-D-1 and ISOS-D-3 respectively), laboratory weathering tests (intermediate and advanced levels, ISOS-L-2, ISOS-L-3) and outdoor (ISOS-O-1) testing were performed. Table 3 show the initial and final efficiencies of all samples before and after the ageing tests.

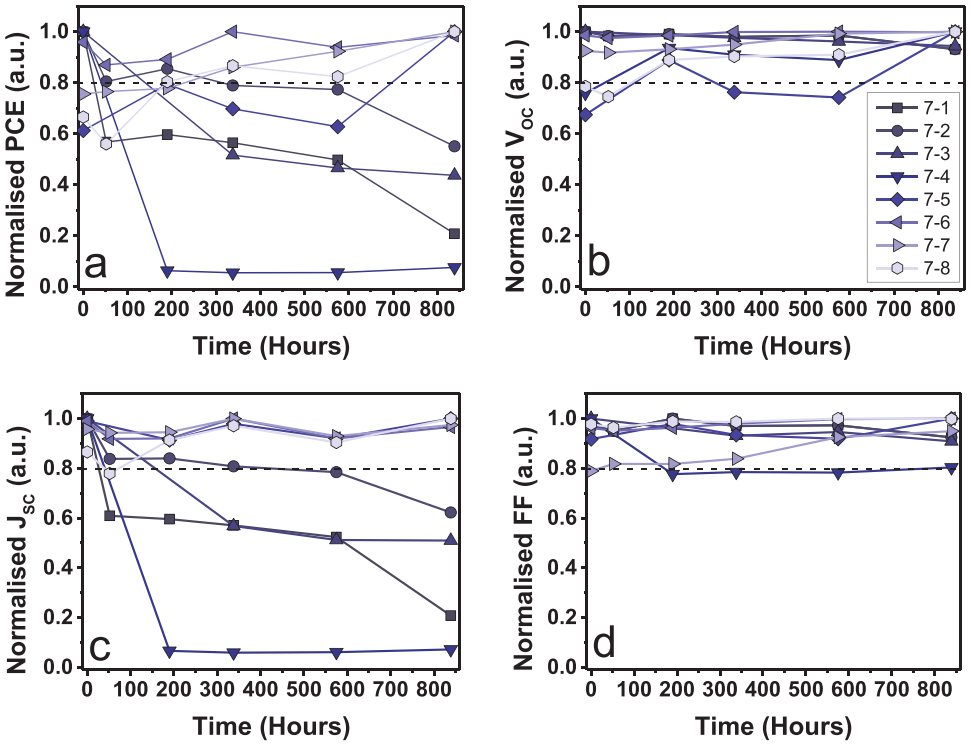

Fig. 6. Normalised a) PCE; b) V_{OC}; c) J_{SC}; and d) FF vs time plot after 840 h of ISOS-D-1 testing for **P-SBTBDT** solar cell module.

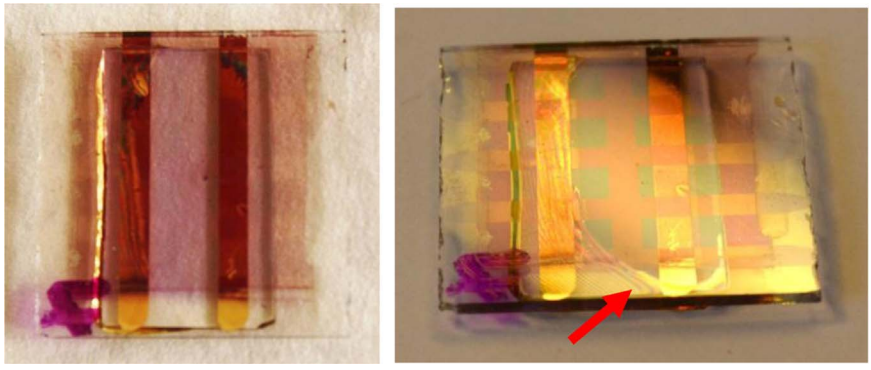

Fig. 7. Photographs of the **P-SBTBDT** OPV module number 7 after ISOS-D-1 test for 840 h. Left: View from the top; right: view with an angle that makes it possible to see the damaged encapsulation (arrow indication) and the ITO layers.

3.3. ISOS-D-1 experiment

ISOS-D-1 shelf life test where performed by storing the samples in ambient atmosphere in a drawer. The stability performances of the samples are shown in Fig. 6a, which reveals that the devices 7-6 and 7-7 remained very stable for 35 days (840 h). Encapsulation problems were observed in cells 7-1 to 7-4 which showed rapid degradation (catastrophic failure). The encapsulation method used is very simple method. UV epoxy resin was applied onto the device by a pastor pipette. Then it is closed with a glass then exposed to UV light for few minutes. During encapsulation process the amount of epoxy resin may change slightly. Also the UV epoxy resin was not dispersed very well; some sites were encapsulated better than some others. Hence, some devices are more durable than the others. Meanwhile the samples 7-5 and 7–8 originally had a rather low performance (see Table 3) possibly due to the damage in the active area (to be discussed below) and therefore the ageing curves resulted in unconventional gradual increasing or fluctuating shape. V_{OC} and FF remained rather constant throughout the tests indicating that the failures were mostly associated with the failure of free carrier generation within the active layer.

In Fig. 7 the P-SBTBDT solar cell number 7 is illustrated. From the right image it is easy to spot that the encapsulation adhesive has shrank leaving the large part of the cells expose to air, which explains the rapid failure of these samples as mentioned before (cells 7.1 and 7.4). The numbering of the cells can be seen from Fig. 1. In the left photograph on the right stripe visible active layer defects can be identified in cells 7-5 and 7–8, which explain the initial low performance.

3.4. ISOS-D-3 experiment

The damp heat test ISOS-D-3 was carried out at high temperature 65 °C and 85% relative humidity.

The results showed that all devices, after a burning-in phase of approximately 50 h, remained stable for at least 350 h which is

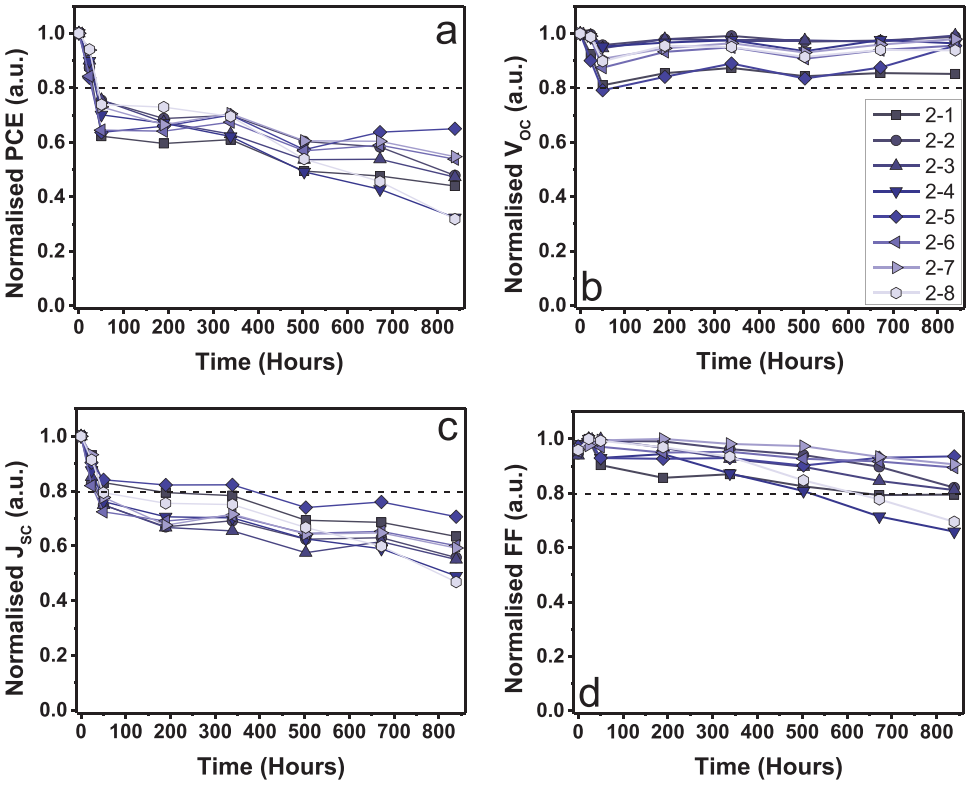

Fig. 8. Normalised a) PCE; b) V_{OC}; c) J_{SC}; and d) FF vs time plot after 840 h of ISOS-D-3 testing for **P-SBTBDT** solar cell module.

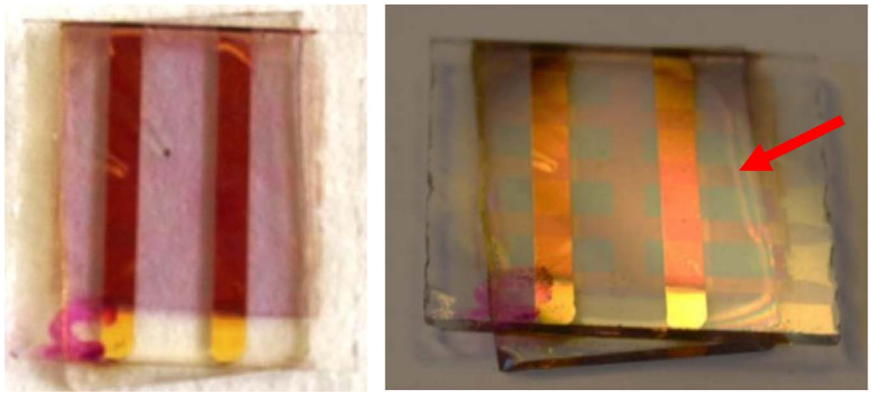

Fig. 9. Photographs of the **P-SBTBDT** OPV module number 2 after ISOS-D-3 test for 840 h. Left: View from the top; right: view with an angle that makes possible to see the encapsulation damaged (arrow indication) and the ITO layers.

remarkable even for encapsulated devices under ISOS-D-3 test (Fig. 8a) [39]. Cells 2–4 and 2–8 had a more accentuated degradation since they were closer to the edges than the others. Fabrication defects possibly had a negative effect on the performance of cells 2-2 and 2–3. The devices were still working with around 70 to 50% of their initial performances by the end of the test. The V_{OC} remained rather constant (Fig. 8b) in contrast to J_{SC} and FF, which degraded gradually (Fig. 8c and d). Although the burn-in phase had a strong effect in the modules performance, this study indicated that P-SBTBDT is rather stable and robust polymer even when exposed to high temperatures and humidity. Images of OPV devices after ISOS-D-3 testing (Fig. 9) revealed a fabrication defect in the active layer between cell 2-2 and 2–3, and a slight alteration in the encapsulation at the edges, especially on the top part of the module, close to cells 2–4 and 2–8.

3.5. *ISOS-L-2 experiment*

Laboratory light soaking test (ISOS-L-2) was also carried out with 2 modules at monitored 65 °C device temperature under solar simulator. This test is considered as accelerated aging due to harsh conditions. In the experiment, the samples are subjected to both elevated temperature and continuous light exposure which significantly affect the sample lifetime.

The results of ISOS-L-2 testing revealed that the devices degraded very fast under solar light and at high temperature (Fig. 10a). One of the devices (1-1) maintains around 40% of its initial performance until 338 h and another (1–3) stabilizes at 20% after the burn-in phase. Temperature exhibits an accelerating effect on the degradation of the devices with sunlight compared to ISOS-L-1 (Fig. 5). T_{80} value of about 68 h was recorded in ISOS-L-1 test, while only 6–13 h were observed in

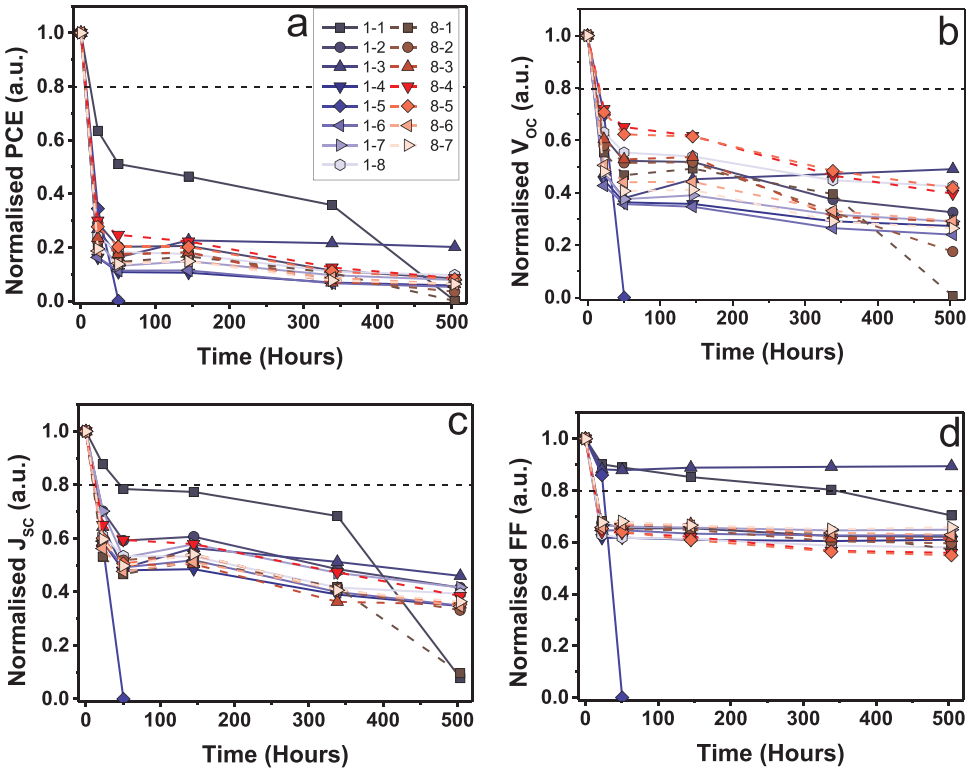

Fig. 10. Normalised a) PCE; b) V_{OC}; c) J_{SC}; and d) FF vs time plot after 500 h of ISOS-L-2 testing for **P-SBTBDT** solar cell modules.

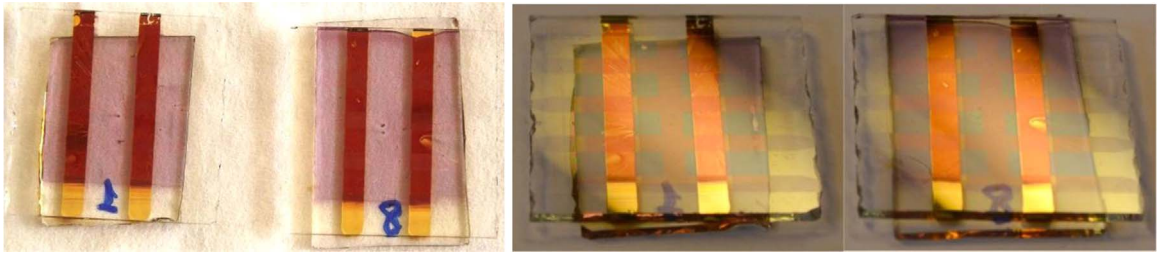

Fig. 11. Photographs of the **P-SBTBDT** OPV modules number 1 and 8 after ISOS-L-2 test for 500 h. Left: View from the top; right: view with an angle that makes possible to see the encapsulation and the ITO layers.

the case of ISOS-L-2 due to additionally elevated temperatures. Complete failure was detected for devices 1–4 and 8-1. Degradation of V_{OC} (Fig. 10b) together with J_{SC} and FF (Fig. 10c and b) suggested possible chemical changes in the active layer resulting in energy level modifications. In the modules photograph (Fig. 11) there was no sign of encapsulation defects in the modules, indicating that degradation was mainly provoked by light and temperature effects. A fabrication defect could be seen in cell 8-6, although the cell degradation behavior followed the average of the other cells.

The high temperature annealing with light exposure (ISOS-L-2) led to the worst result, since ultraviolet radiation may cause significant degradation of polymeric materials. UV radiation leads to photo-oxidative degradation which results in breaking of the polymer chains, produces radicals and reduces the molecular weight. This causes deterioration of mechanical properties leading to the production of useless materials after an unpredictable time. Our AFM results also revealed that photooxidation causes higher degradation than the ISOSD3 test.

3.6. ISOS-L-3 experiment

ISOS-L-3 is the harshest test where the samples are exposed to light, elevated temperature of 65 °C and 50% humidity. The test was performed on two modules and as expected the samples showed fast degradation.

Fig. 12a shows that the devices again experienced an accentuated burn-in phase, similar to the one in ISOS-L-2, but less intense corresponding to the less intensive light source (0.7 sun). In general the module number 4 had a higher average stabilization of the devices after the burn-in. Module number 6 clearly showed that there was encapsulation issues during the aging, Nevertheless, devices 6-5 and 6-6 (with T_{80} 42 and 79 h respectively defined in the stabilized phased of the curve) are exceptions and degraded slower than all the other cells in module 6 and 4. Cells 6-1, 6–7 and 6–8 had complete failure during the test. In the module 4, which had less issues concerning the encapsulation, the behavior of V_{OC}, J_{SC} and FF (Fig. 12b, c and d) under ISOS-L-3

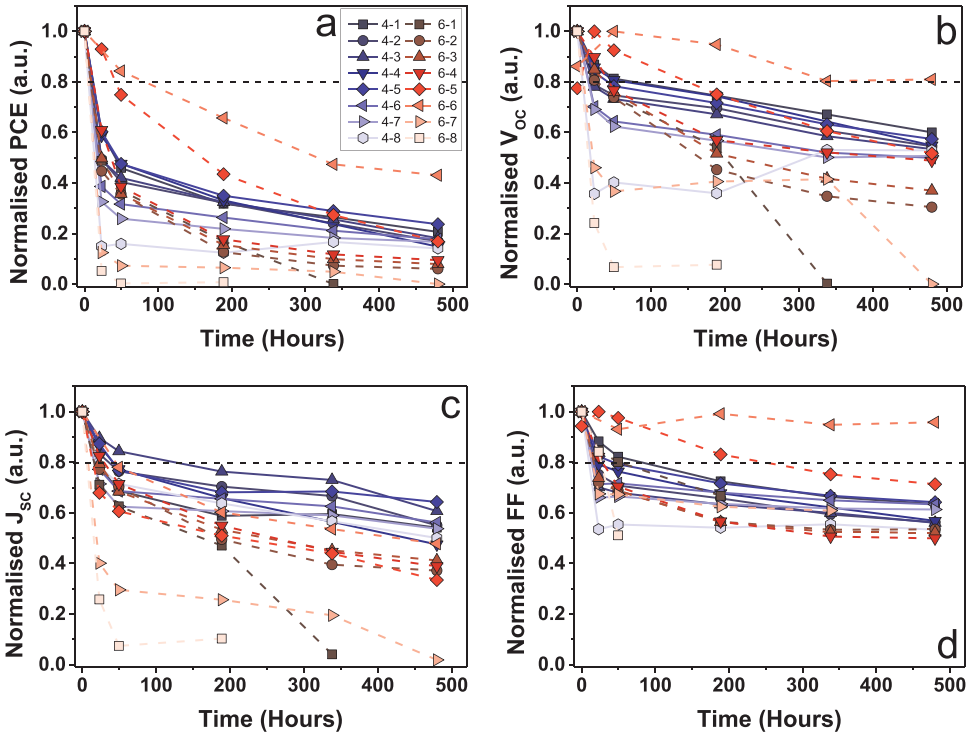

Fig. 12. Normalised a) PCE; b) V_{OC}; c) J_{SC}; and d) FF vs time plot after 480 h of ISOS-L-3 testing for **P-SBTBDT** solar cell modules.

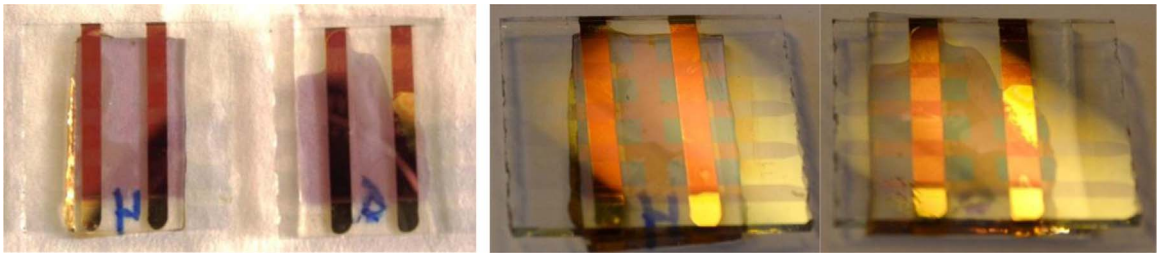

Fig. 13. Photographs of the **P-SBTBDT** OPV modules number 4 and 6 after ISOS-L-3 test for 480 h. Left: View from the top; right: view with an angle that makes possible to see the encapsulation and the ITO layers.

were very similar to those of ISOS-L-2, with significantly less intense burn-in. The 50% relative humidity applied during this test seemed not to have a big role in the degradation mechanism of P-SBTBDT solar cells, apart from the ones with encapsulation issues. Images of the modules (Fig. 13) revealed that the active layer was severely damaged during the test in module 6, corresponding to the failure and odd behavior of the devices performance. When ISOS-L-1, ISOS-L-2 and ISOS-L-3 tests are compared, the addition of humidity in ISOS-L-3 test did not cause any major change in the degradation behavior, as expected after the low degradation levels presented in ISOS-D-3 which had 85% relative humidity.

3.7. ISOS-O-1 experiment

To address the correspondence of indoor simulations and outdoor stability, ISOS-O-1 was performed on modules 3 and 5. Normalised efficiency vs time plot (Fig. 14a) showed catastrophic failure of several cells after 300 h, and total failure of most of them by the end of the test in module 5. Cells 3-1, 3-2 and 3-3 were the ones that didn't show marked encapsulation or fabrication defects. These devices had less pronounced burn-in phase compared to the indoor tests, with T_{80} values ranging between 36 and 46 h. The samples degraded linearly until 500 h and had a more stable phase until the end of the test. The aging curves for V_{OC}, J_{SC} and FF (Fig. 14b, c and d) follow similar behavior, as in the indoors light tests, showing again the sensitivity of the devices (and active layer) to light and temperature, although much less harshly. These 3 devices remained with around 40% of their initial performance after 840 h of outdoor exposure. Device 5-1 ended up with the same normalised performance with a slight difference during the aging. The photographs of the samples taken by the end of the test show the severe damage in the encapsulation and the active layer in both devices after outdoor exposure. Only the region of cell 3-1 to 3-3 and barely cell 5-1 remained intact (Fig. 15).

3.8. Morphology Investigation of P-SBTBDT:PCBM blends after stability testing

To investigate the morphology changes for P-SBTBDT:PCBM films for ISOSL1 and ISOSD3 stability tests, AFM images of the blends were taken after ISOS stability tests at different time intervals. AFM photos of

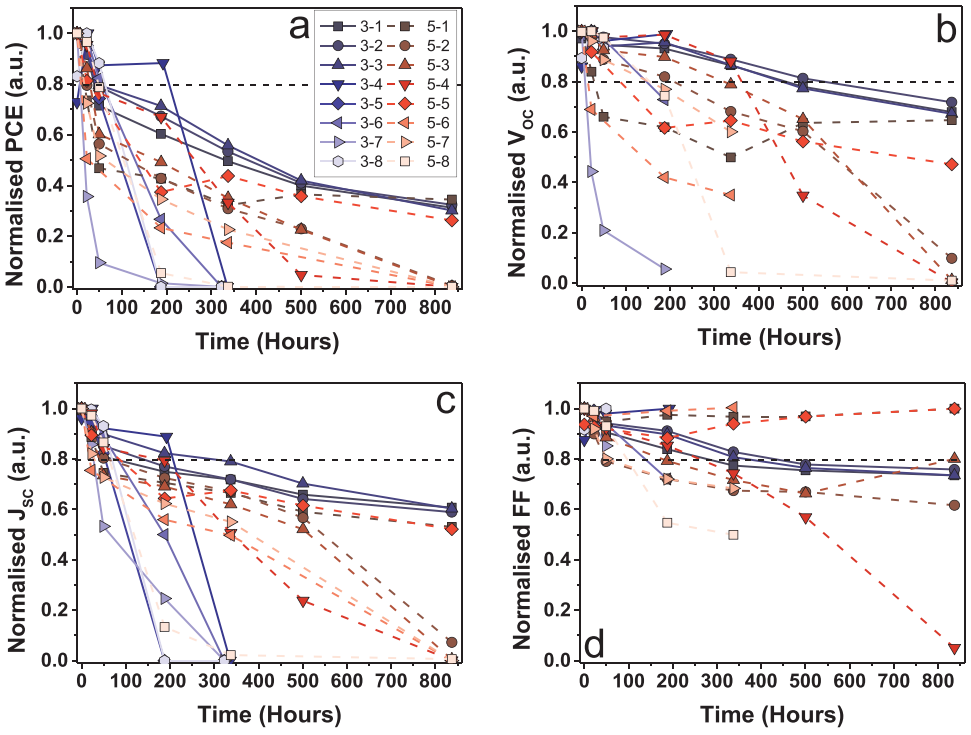

Fig. 14. Normalised a) PCE; b) V_{OC}; c) J_{SC}; and d) FF vs time plot after 840 h of ISOS-O-1 testing for **P-SBTBDT** solar cell modules.

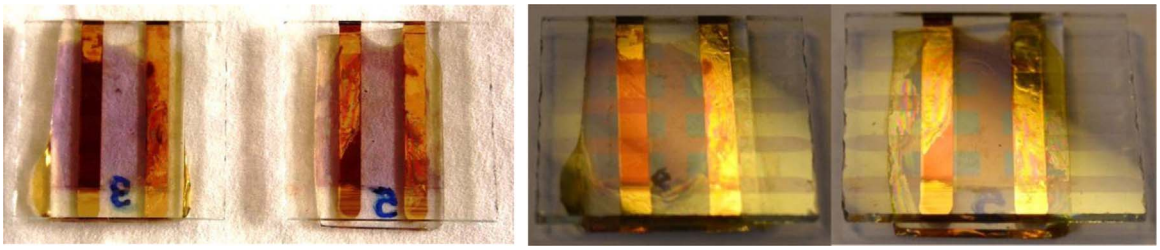

Fig. 15. Photographs of the **P-SBTBDT** OPV modules number 3 and 5 after ISOS-O-1 test for 840 h. Left: View from the top; right: view with an angle that makes possible to see the encapsulation damaged and the ITO layers.

P-SBTBDT:PCBM films were taken without any treatment; roughness was about 5 nm. Besides, some aggregation appeared that is triangular shaped with a size of 0.5 μm (Fig. 16a). After 48 h ISOSL1 and ISOSD3 tests, roughness values decreased by 1.50 and 1.80 nm respectively (Fig. 16b-c). Solar irradiation and heat exposure led to a positive effect on the morphology of the films for 48 h. However, ISOSD3 results showed that some pinholes (≅ 150 nm) appeared after 48 h. After 96 h ISOSL1 and ISOSD3 test indicated that roughness were increased by 2.80 and 4.10 nm respectively. ISOSD3 test showed bigger pinholes (≅ 200 nm) for 96 h (Fig. 16d-e). After 120 h ISOSL1 and ISOSD3 test indicated that roughness were increased by 3.30 and 6 nm respectively (Fig. 16f-g). That brings out roughness increased increasing time period of the tests. Finally, ISOSL1 test showed morphology abruptly changed after 450 h, size of aggregation rised (≅ 250 nm) (Fig. 16h) Roughness increased up to ≅ 60 nm, the color of polymer almost disappeared. It is revealed that P-SBTBDT solar cells were affected by solar irradiation significantly; due to photo oxidation of polymer. It can be concluded that photo oxidation is the main reason of P-SBTBDT degradation.

4. Conclusion

In this work the P-SBTBDT solar cell responses under 6 different ISOS conditions were presented. Shelf life (ISOS-D-1) showed that P-SBTBDT solar cell was stable for 840 h. Although ISOS-D-3 has very harsh aging conditions, P-SBTBDT solar cells preserved 50–70% of their initial performance after 840 h, as expected with the inverted architecture of these modules which do not contain moisture sensitive layers. Comparison among basic, intermediate, advanced light tests (ISOS-L-1, ISOS-L-2, ISOS-L-3) and dark tests (ISOS-D-1 and ISOS-D-3) showed sensitivity of the devices to air, light and temperature. Nevertheless, a remarkable stability was observed under damp heat conditions (ISOS-D-3) and confirmed by comparing the light indoor tests with and without humidity. Outdoor tests showed that indoor tests provoked much more severe degradation in the modules.

Voc is affected by the HOMO level of donor an LUMO level of acceptor, it is a parameter depending on the nature of polymers. Kumar et al. [40] studied stability and reliability of P3HT inverted solar cell, it was indicated that Voc values of the cells were affected slightly during

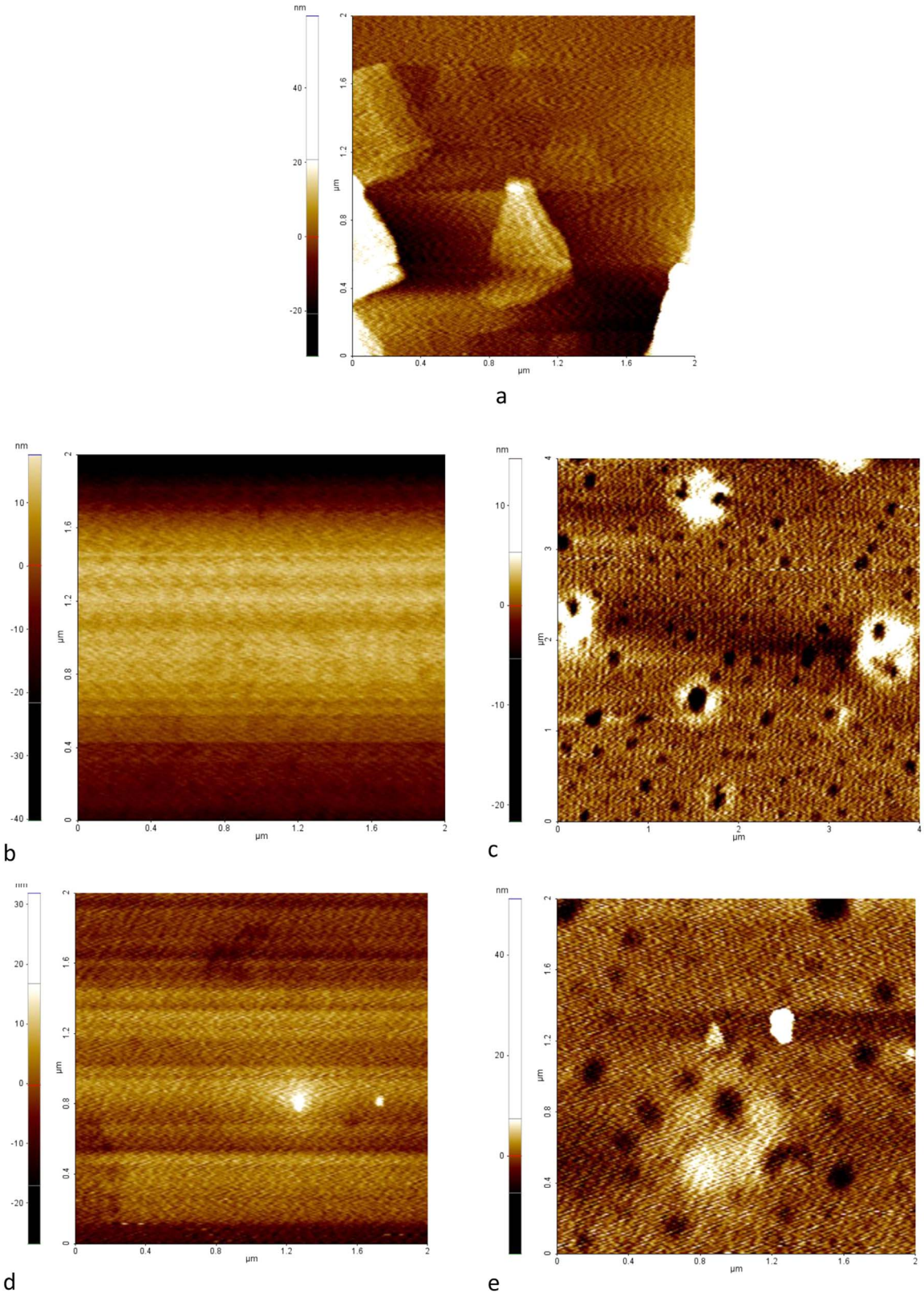

Fig. 16. AFM images of P-SBTBDT:PCBM solar cells exposed to ISOSL1 and ISOS D3 tests after different time periods; a) reference solar cell, b) after 48 h at ISOSL1, c) after 48 h at ISOSD3, d) after 96 h at ISOSL1, e) after 96 h at ISOSD3,f) after 120 h at ISOSL1, g) after 120 h at ISOSD3, h) after 450 h at ISOSL1, i) after 450 h at ISOSD3.

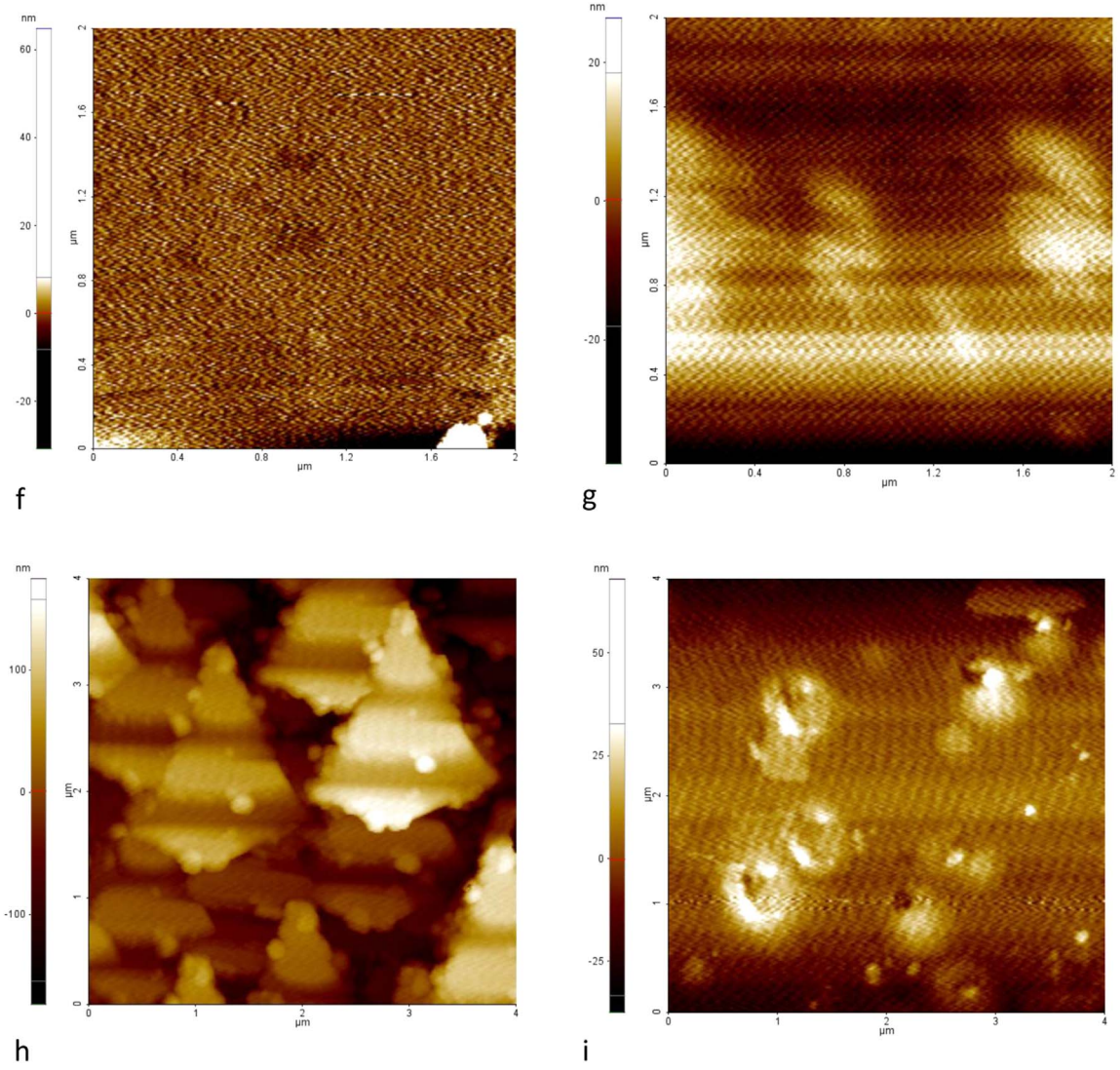

Fig. 16. (*continued*)

stability tests. Our stability tests also show that Voc values are mildly affected during stability tests.

Even though advanced encapsulation techniques were not used, the inverted P-SBTBDT solar cells were found to be very stable under damp conditions and further improvement can be addressed towards light, oxygen and heat resistance. As the next step, different deposition techniques, such as atomic layer deposition (ALD) will be used as well as specific barrier layers in order to improve the stability of P-SBTBDT solar cells.

References

[1] F.C. Krebs, Low band gap polymer materials for organic solar cells, Sol. Energy Mater. Sol. Cells 91 (2007) 953.
[2] H. Spanggaard, F.C. Krebs, A brief history of the development of organic and polymeric photovoltaics, Sol. Energy Mater. Sol. Cells 83 (2004) 125–146.
[3] F. Krebs, The Development of Organic and Polymer Photovoltaics, Elsevier Science, Amsterdam, Netherlands, 2004 (PO BOX 211, 1000 AE).
[4] E.A. Parlak, The blend ratio effect on the photovoltaic performance and stability of poly (3-hexylthiophene): [6, 6]-phenyl-C 61 butyric acid methyl ester (PCBM) and poly (3-octylthiophene): pcbm solar cells, Sol. Energy Mater. Sol. Cells 100 (2012) 174–184.
[5] C.-H. Hsieh, Y.-J. Cheng, P.-J. Li, C.-H. Chen, M. Dubosc, R.-M. Liang, C.-S. Hsu, Highly efficient and stable inverted polymer solar cells integrated with a cross-linked fullerene material as an interlayer, J. Am. Chem. Soc. 132 (2010) 4887–4893.
[6] M. Giannouli, V.M. Drakonakis, A. Savva, P. Eleftheriou, G. Florides, S.A. Choulis, Methods for improving the lifetime performance of organic photovoltaics with low-costing encapsulation, ChemPhysChem 16 (2015) 1134–1154.
[7] N. Grossiord, J.M. Kroon, R. Andriessen, P.W. Blom, Degradation mechanisms in organic photovoltaic devices, Org. Electron. 13 (2012) 432–456.
[8] M. Jørgensen, K. Norrman, F.C. Krebs, Stability/degradation of polymer solar cells, Sol. Energy Mater. Sol. Cells 92 (2008) 686–714.
[9] Z. Xu, L.M. Chen, G. Yang, C.H. Huang, J. Hou, Y. Wu, G. Li, C.S. Hsu, Y. Yang, Vertical phase separation in poly (3-hexylthiophene): fullerene derivative blends and its advantage for inverted structure solar cells, Adv. Funct. Mater. 19 (2009) 1227–1234.
[10] J. Huang, G. Li, Y. Yang, A semi-transparent plastic solar cell fabricated by a lamination process, Adv. Mater. 20 (2008) 415–419.
[11] P. Kumar, S. Chand, Recent progress and future aspects of organic solar cell, Prog. Photovol.:Res. Appl. 20 (2012) 377–415.
[12] O. Haillant, Accelerated weathering testing principles to estimate the service life of organic PV modules, Sol. Energ. Mat. Sol. C 95 (2011) 1284–1292.
[13] N. Grossiord, J.M. Kroon, R. Andriessen, P.W.M. Blom, Degradation mechanisms in organic photovoltaic devices, Org. Electron. Devices, Org. Electron. 13 (2012) 432–456.
[14] B. Zimmermann, U. Würfel, M. Niggeman, Longterm stability of efficient inverted P3HT:PCBM solar cells, Sol. Energ. Mat. Sol. C 93 (2009) 491–496.
[15] K. Lee, J.Y. Kim, S.H. Park, S.H. Kim, S. Cho, A.J. Heeger, Air-stable polymer electronic devices, Adv. Mater. 19 (2007) 2445–2449.
[16] J. Gilot, I. Barbu, M.M. Wienk, R.A. Janssen, The use of ZnO as optical spacer in polymer solar cells: theoretical and experimental study, Appl. Phys. Lett. 91 (2007) 113520.
[17] C. Yang, J.Y. Kim, S. Cho, J.K. Lee, A.J. Heeger, F. Wudl, Functionalized methanofullerenes used as n-type materials in bulk-heterojunction polymer solar cells and in field-effect transistors, J. Am. Chem. Soc. 130 (2008) 6444–6450.
[18] J.Y. Kim, S.H. Kim, H.H. Lee, K. Lee, W. Ma, X. Gong, A.J. Heeger, New architecture for high-efficiency polymer photovoltaic cells using solution-based titanium oxide as an optical spacer, Adv. Mater. 18 (2006) 572–576.
[19] Y. Şahin, S. Alem, R. de Bettignies, J.-M. Nunzi, Development of air stable polymer

solar cells using an inverted gold on top anode structure, Thin Solid Films 476 (2005) 340–343.
[20] G. Li, C. Chu, V. Shrotriya, J. Huang, Y. Yang, Efficient inverted polymer solar cells, Appl. Phys. Lett. 88 (2006) (253503-253503).
[21] S.K. Hau, H.-L. Yip, O. Acton, N.S. Baek, H. Ma, A.K.-Y. Jen, Interfacial modification to improve inverted polymer solar cells, J. Mater. Chem. 18 (2008) 5113–5119.
[22] S.K. Hau, H.-L. Yip, N.S. Baek, J. Zou, K. O'Malley, A.K.-Y. Jen, Air-stable inverted flexible polymer solar cells using zinc oxide nanoparticles as an electron selective layer, Appl. Phys. Lett. 92 (2008) 253301.
[23] C. Waldauf, M. Morana, P. Denk, P. Schilinsky, K. Coakley, S. Choulis, C. Brabec, Highly efficient inverted organic photovoltaics using solution based titanium oxide as electron selective contact, Appl. Phys. Lett. 89 (2006) 233517.
[24] M. White, D. Olson, S. Shaheen, N. Kopidakis, D.S. Ginley, Inverted bulk-heterojunction organic photovoltaic device using a solution-derived ZnO underlayer, Appl. Phys. Lett. 89 (2006) 143517.
[25] B.-Y. Yu, A. Tsai, S.-P. Tsai, K.-T. Wong, Y. Yang, C.-W. Chu, J.-J. Shyue, Efficient inverted solar cells using TiO2 nanotube arrays, Nanotechnology 19 (2008) 255202.
[26] G.K. Mor, K. Shankar, M. Paulose, O.K. Varghese, C.A. Grimes, High efficiency double heterojunction polymer photovoltaic cells using highly ordered TiO2 nanotube arrays, Appl. Phys. Lett. 91 (2007) 2111.
[27] H.-H. Liao, L.-M. Chen, Z. Xu, G. Li, Y. Yang, Highly efficient inverted polymer solar cell by low temperature annealing of Cs2CO3 interlayer, Appl. Phys. Lett. 92 (2008) (173303-173303).
[28] Y. Dong, X. Hu, C. Duan, P. Liu, S. Liu, L. Lan, D. Chen, L. Ying, S. Su, X. Gong, A series of new medium-bandgap conjugated polymers based on naphtho [1, 2-c: 5, 6-c] bis (2-octyl-[1, 2, 3] triazole) for high-performance polymer solar cells, Adv. Mater. 25 (2013) 3683–3688.
[29] K. Li, Z. Li, K. Feng, X. Xu, L. Wang, Q. Peng, Development of large band-gap conjugated copolymers for efficient regular single and tandem organic solar cells, J. Am. Chem. Soc. 135 (2013) 13549–13557.
[30] S.C. Price, A.C. Stuart, L. Yang, H. Zhou, W. You, Fluorine substituted conjugated polymer of medium band gap yields 7% efficiency in polymer− fullerene solar cells, J. Am. Chem. Soc. 133 (2011) 4625–4631.
[31] A. Patra, M. Bendikov, Polyselenophenes, J. Mater. Chem. 20 (2010) 422–433.
[32] H.-Y. Chen, S.-C. Yeh, C.-T. Chen, C.-T. Chen, Comparison of thiophene-and selenophene-bridged donor–acceptor low band-gap copolymers used in bulk-heterojunction organic photovoltaics, J. Mater. Chem. 22 (2012) 21549–21559.
[33] B. Kim, H.R. Yeom, M.H. Yun, J.Y. Kim, C. Yang, A selenophene analogue of PCDTBT: selective fine-tuning of LUMO to lower of the bandgap for efficient polymer solar cells, Macromolecules 45 (2012) 8658–8664.
[34] D.H. Wang, A. Pron, M. Leclerc, A.J. Heeger, Additive-free bulk-heterojuction solar cells with enhanced power conversion efficiency, comprising a newly designed selenophene-thienopyrrolodione copolymer, Adv. Funct. Mater. 23 (2013) 1297–1304.
[35] M.O. Reese, S.A. Gevorgyan, M. Jørgensen, E. Bundgaard, S.R. Kurtz, D.S. Ginley, D.C. Olson, M.T. Lloyd, P. Morvillo, E.A. Katz, Consensus stability testing protocols for organic photovoltaic materials and devices, Sol. Energy Mater. Sol. Cells 95 (2011) 1253–1267.
[36] H. Unay, N.A. Unlu, G. Hizalan, S.O. Hacioglu, D.E. Yildiz, L. Toppare, A. Cirpan, Benzotriazole and benzodithiophene containing medium band gap polymer for bulk heterojunction polymer solar cell applications, J. Polym. Sci. Part A: Polym. Chem. 53 (2015) 528–535.
[37] S.A. Gevorgyan, M.V. Madsen, B. Roth, M. Corazza, M. Hösel, R.R. Søndergaard, M. Jørgensen, F.C. Krebs, Lifetime of organic photovoltaics: status and predictions, Adv. Energy Mater. (2015).
[38] J.E. Carlé, M. Helgesen, M.V. Madsen, E. Bundgaard, F.C. Krebs, Upscaling from single cells to modules–fabrication of vacuum-and ITO-free polymer solar cells on flexible substrates with long lifetime, J. Mater. Chem. C 2 (2014) 1290–1297.
[39] M. Corazza, F.C. Krebs, S.A. Gevorgyan, Predicting, categorizing and intercomparing the lifetime of OPVs for different ageing tests, Sol. Energy Mater. Sol. Cells 130 (2014) 99–106.
[40] N. Chander, S. Singh, S.S. Kumar, Sol. Energy. Sol. Cells 161 (2017) 407–415.